Nanoindentation of Lemur Enamel: An Ecological Investigation of Mechanical Property Variations Within and Between Sympatric Species

Sara E. Campbell,[1] Frank P. Cuozzo,[2] Michelle L. Sauther,[3] Matt Sponheimer,[3] and Virginia L. Ferguson[1]*

[1]*Department of Mechanical Engineering, University of Colorado, Boulder, CO 80309*
[2]*Department of Anthropology, University of North Dakota, Grand Forks, ND 58202*
[3]*Department of Anthropology, University of Colorado, Boulder, CO 80309*

ABSTRACT   The common morphological metrics of size, shape, and enamel thickness of teeth are believed to reflect the functional requirements of a primate's diet. However, the mechanical and material properties of enamel also contribute to tooth function, yet are rarely studied. Substantial wear and tooth loss previously documented in *Lemur catta* at the Beza Mahafaly Special Reserve suggests that their dental morphology, structure, and possibly their enamel are not adapted for their current fallback food (the mechanically challenging tamarind fruit). In this study, we investigate the nanomechanical properties, mineralization, and microstructure of the enamel of three sympatric lemur species to provide insight into their dietary functional adaptations. Mechanical properties measured by nanoindentation were compared to measurements of mineral content, prism orientation, prism size, and enamel thickness using electron microscopy. Mechanical properties of all species were similar near the enamel dentin junction and variations correlated with changes in microstructure (e.g., prism size) and mineral content. Severe wear and microcracking within *L. catta's* enamel were associated with up to a 43% reduction in nanomechanical properties in regions of cracking versus intact enamel. The mechanical and material properties of *L. catta's* enamel are similar to those of sympatric folivores and suggest that they are not uniquely mechanically adapted to consume the physically challenging tamarind fruit. An understanding of the material and mechanical properties of enamel is required to fully elucidate the functional and ecological adaptations of primate teeth. Am J Phys Anthropol 148:178–190, 2012.   © 2012 Wiley Periodicals, Inc.

A long history of research, from almost two centuries of work, illustrates that mammalian teeth are generally adapted for an organism's diet (Teaford, 2000; Lucas, 2004; Ungar, 2010). However, examples from living mammals, from the fossil record, and even human paleobiology indicate that this is not always the case (e.g., Lebel and Trinkaus, 2002; Jablonski and Leakey, 2008). The complex structure of the tooth is believed to evolve in response to functional requirements through alteration of tooth shape, size, and enamel thickness (Gregory, 1922; Crompton and Sita-Lumsden, 1970; Kay and Hiiemae, 1974; Maas and Dumont, 1999; Lucas, 2004). Tooth functionality and wear also depend on less commonly explored factors, such as enamel microstructure and mechanical properties (Maas and Dumont, 1999; Lucas, 2004; He and Swain, 2008; Xie et al., 2009; Macho and Shimizu, 2010). Yet, only recently have investigators explored the nanomechanical properties of primate enamel (Mahoney et al., 2000; Cuy et al., 2002; He and Swain, 2008; Darnell et al., 2010; Lee et al., 2010; see Table 1).

Thick enamel has been linked to hard object feeding in primates (Kay, 1981; Dumont, 1995) and has been suggested to provide greater wear potential (Macho and Spears, 1999) or resistance to fracture (Kay, 1981; Lucas et al., 2008). However, the relationship between thick enamel and hard object consumption is not direct (Maas and Dumont, 1999; Teaford and Ungar, 2000; Martin et al., 2003). New World pithecine primates have thin enamel with considerable prism decussation, yet are able to successfully consume hard objects, indicating that enamel microstructure plays a vital role in the function of the tooth (Martin et al., 2003; Macho and Shimizu, 2009, 2010). Furthermore, the functionality of the tooth directly depends on the mechanical properties of enamel that have been linked to a number of material properties including: prism orientation, mineralization, microstructure, and composition (Cuy et al., 2002; Angker et al., 2004; Shimizu and Macho, 2008; Xie et al., 2009). Thus, investigation of enamel's mechanical and material properties, in addition to more traditional studies of tooth morphology, will likely improve our understanding of dental ecology and tooth functionality.

The ring-tailed lemurs (*Lemur catta*) of the riverine gallery forests of southern Madagascar, where the only long-term ecological studies of this species have occurred [see chapters in Jolly et al. (2006)], rely heavily on a hard, tough fallback fruit from the tamarind tree, *Tamarindus indica* (Yamashita, 1996, 2002, 2003; Sauther, 1998; Cuozzo and Sauther, 2004, 2006; Simmen et al., 2006;

TABLE 1. Comparison of mechanical properties of primate enamel using nanoindentation testing

Species (common name, sample n)	Tooth (location)	Modulus ± STD (GPa)	Hardness ± STD (GPa)	Test method
Homo sapiens[a] (human, 3)	M[2] (EDJ to OS)	47–120	2.7–6.4	800 nm
Alouatta palliata[b] (howler monkey, 1)	M[1] (EDJ)	77.3 ± 7.4	4.75 ± 0.70	600 nm
Lepilemur leucopus[c] (sportive lemur, 2)	M[2] (EDJ ½)	78.2 ± 4.9	4.25 ± 0.31	50 mN
Homo sapiens[d] (human, 8)	M[1] (100 µm above EDJ)	80.4 ± 7.7	4.88 ± 0.35	50 mN
Alouatta palliata[b] (howler monkey, 1)	M[3] (EDJ)	85.2 ± 9.7	4.13 ± 0.30	600 nm
Lemur catta[c] (ring-tailed lemurs, 2)	M[2] (EDJ ½)	88.3 ± 2.8	4.43 ± 0.19	50 mN
Propithecus verreauxi[c] (Verreaux's sifaka, 2)	M[2] (EDJ ½)	87.4 ± 3.4	4.13 ± 0.28	50 mN
Homo sapiens[c] (human, 2)	M[2] (EDJ ½)	88.7 ± 3.4	4.04 ± 0.27	50 mN
Homo sapiens[e] (human, 1)	M_3 (middle 20%)	90.6 ± 4.6	4.01 ± 0.37	400 nm
Gorilla gorilla[e] (gorilla, 1)	M[1] (middle 20%)	93.0 ± 3.2	4.40 ± 0.20	400 nm
Pan trogldytes[e] (chimpanzee, 1)	M_2 (middle 20%)	104.0 ± 2.8	4.80 ± 0.20	400 nm
Pongo pygmaeus[e] (orangutan,1)	M_2 (middle 20%)	100.3 ± 2.9	4.83 ± 0.23	400 nm

Nanoindentation testing method of either max load or max depth are listed in the last column.
[a] Cuy et al., 2002.
[b] Darnell et al., 2010.
[c] This work.
[d] Mahoney et al., 2000.
[e] Lee et al., 2010. Also see Constantino et al. (submitted) for more nanoindentation of more species.

TABLE 2. Measured and literature values for RET, prism patterns (PP), and prism width (PW) indicating the presence of Hunter-Schreger bands (HSB)

Taxon	Worn-RET mean (std)	RET Lit. mean (n), range	Observed PP (HSB)	Lit. PP (HSB)	PW (µm) mean(std)	Body mass (g)	Diet
H. sapiens	Sample 1 = 29.09 (0.18) Sample 2 = 25.92 (0.15)	22.4 (13)[a] 13.8–32.3	3 (HSB)	1, 2, 3 (HSB)[b,c]	6.33 (0.62)	>40,000[d]	Processed foods
L. catta	Sample 1 = 4.09 (0.02) Sample 2 = 3.49 (0.08)	6.7–8.1[e]	3 (HSB)	1, 3 (HSB)[f]	4.47 (0.37)	~2210[f,g]	Fruit, wild figs, leaves, herbs, flowers[h,i,j,k]
P. verreauxi[l]	Sample 1 = 11.78 (0.09) Sample 2 = 7.89 (0.56)	10.7[e]	3 (HSB)	1, 3 (HSB)[f]	4.49 (0.71)	~3000[g,h]	Leaves, flowers, bark, some fruit[h,i,m,n]
L. leucopus	Sample 1 = 16.47 (0.18) Sample 2 = 15.23 (0.19)	N.A.	3 (no HSB)		3.87(0.33)	~540[o,p]	Leaves, stems, flowers, cecotroph[q,r]

Additionally, literature (lit.) values for the mass and observed diet of each species are listed.
[a] Martin, 1985.
[b] Martin et al., 1988.
[c] Boyde and Martin, 1982.
[d] Fleagle, 1998.
[e] Godfrey et al., 2005.
[f] Maas, 1994.
[g] Kay, 1975.
[h] Jolly, 1967.
[i] Rand, 1935.
[j] Shaw, 1879.
[k] Sussman, 1974.
[l] Malagasy strepsirrhine taxa.
[m] Hill, 1954.
[n] Forbes, 1894.
[o] Harcourt and Thornback, 1990.
[p] Tattersall, 1982.
[q] Nash, 1998.
[r] Schoeninger et al., 1998.

Sauther and Cuozzo, 2009). *Lemur catta* has extremely thin enamel compared to other primates (see Table 2; Shellis et al., 1998; Martin et al., 2003; Godfrey et al., 2005). Consumption of this mechanically challenging fallback food contributes to extreme tooth wear and frequent tooth loss (Sauther et al., 2002; Cuozzo and Sauther, 2004, 2006). This damage suggests that *L. catta* enamel is not equipped to handle the high stresses associated with its diet at this locality. As seen in previous work on this population (Cuozzo and Sauther, 2006; Millette et al.,

2009; Sauther and Cuozzo, 2009), there appears to be an anatomical mismatch (e.g., evolutionary disequilibrium) between the dental morphology (e.g. thin enamel) of this species, and its primary fallback food. Sauther and Cuozzo (2009) suggest that this disequilibrium is in part a product of the dramatic changes to Madagascar's fauna and environment over the past two millennia.

Although *L. catta*'s extreme tooth wear has been studied from a morphological perspective, little is known about the material properties of its enamel. It is possible

that variations in enamel microstructure or mechanical properties mitigate the impact of *L. catta*'s thin enamel. In this study, we will determine whether the nanomechanical properties, microstructure, and mineralization of *L. catta*'s enamel are substantially different from two sympatric species, indicating that *L. catta* is not uniquely adapted to consumption of its hard and tough fallback food.

MATERIALS AND METHODS

The maxillary second molar (M^2) was sampled from two adults from three lemur species (*Lepilemur leucopus*, *L. catta*, and *Propithecus verreauxi*) and *Homo sapiens*. Lemur samples were obtained from naturally deceased animals at the Beza Mahafaly Special Reserve, southwestern Madagascar (23° 30′ S latitude, 44° 40′ E longitude) by the authors Cuozzo, FP (FPC) and Sauther, ML (MLS). Specimens were collected from the Beza Mahafaly reserve forest in 1987 by MLS, as part of the long-term development and maintenance of a comparative lemur osteological collection. Teeth were removed from the skulls of the six dental adults, after full dental impressions were made to preserve a record of these teeth before the destructive analyses. Teeth from *L. catta* and *P. verreauxi* were noted to have a moderate, nonexcessive, amount of wear compared to the average population at Beza Mahafaly. Additionally, two adult *Homo sapiens* M^2s were supplied by the dental school at the University of Colorado-Boulder. Each tooth was embedded in polymethylmethacrylate (PMMA) under vacuum and then sectioned along the buccal–lingual direction through the mesial cusps, using a low-speed diamond-wafering saw (Isomet: Buehler, Lake Bluff, IL). The low modulus of PMMA contributes minimally to the measured mechanical properties of the samples (Ferguson, 2004). The mesial half was then polished with a series of silicon carbide papers (300, 400, 600, and 1200 grit) and then with successively finer diamond suspension paste (Buehler) of particle size 6, 3, and 0.25 μm. The specimens were ultrasonically cleaned with deionized water to remove polishing debris between each step. As a final preparation, samples were air dried after ultrasonic cleaning for a minimum of 72 h before analysis.

Mechanical testing

Investigation of the nanomechanical properties of enamel within and between species was performed by nanoindentation testing (NANO Indenter XP, MTS Systems Co., Oak Ridge, TN). The enamel of each PMMA-embedded sample was loaded over 30 s to a maximum load of 50 mN (depth $\approx$ 800 nm) using a Berkovich (three-sided pyramidal) tip giving a constant loading rate of 1.667 mN/s. At maximum load, the indenter was held for 30 s to minimize the creep response during unloading allowing measurement of primarily elastic properties. Because biological materials possess inherently time-dependent behavior, it is a common practice to minimize viscous behavior on unloading through an extended creep hold (Ferguson and Olesiak, 2010; Feng and Ngan, 2002). An example of a nanoindentation load-displacement curve is given in Figure 1B. Data were analyzed using a modified version of the "Oliver-Pharr method" (Oliver and Pharr, 1992) to determine Hardness (*H*) and plane strain modulus (hereafter referred to as modulus or *E*′). Plane strain modulus is calculated from
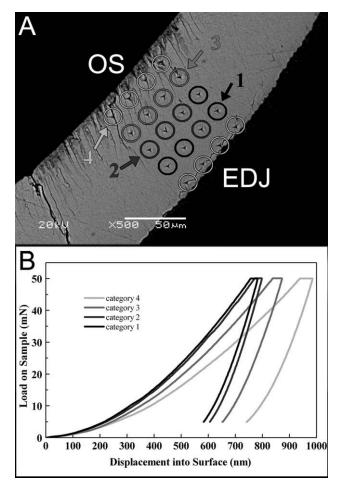

Fig. 1. Image **A** is a BSE image of substantial cracking present in *L. catta* sample 2 demonstrating cracking category classification on an indentation array. The indentation array covers the area from the EDJ (enamel dentin junction) to the OS (occlusal surface). Image **B** provides the load-displacement nanoindentation curves for a representative indent in each cracking category. Nanoindentation data were classified into four categories based on location of indent test site to a microcrack. Category 1 = ideal indent location with no visible damage, Category 2 = indent site is >1 and ≤3 indent widths from a crack, Category 3 = indent site is ≤1 indent width from a crack, and Category 4 = indent is directly on a crack or visible damage.

the slope of the first 80% of the unloading curve, the tip area function A_c (calibrated using a fused silica standard), and the known elastic parameters of the Berkovich tip (given by the Young's modulus and Poisson's ratio of diamond: $E_i = 1140$ GPa and $v_i = 0.07$, respectively) (Oliver and Pharr, 1992). The indentation hardness (*H*) can be determined from the maximum load and the tip area function. All indentation points near a visible crack or void were discarded from this primary data set (category 1).

Indent arrays were four indents wide for all lemur samples (with 20 μm spacing). Array was placed perpendicular to and covering the area from the enamel dentin junction (EDJ) to the occlusal surface (OS). Indent arrays were placed on the two main cusps (or nearby when cusps had been worn away) and through the central valley (see Fig. 2). To cover the entire area from the EDJ to OS lemur teeth required 5–19 rows of indents

depending on enamel thickness at the location of the array. Arrays placed on *Homo sapiens* samples had 50 μm spacing and only three indents per row due to the
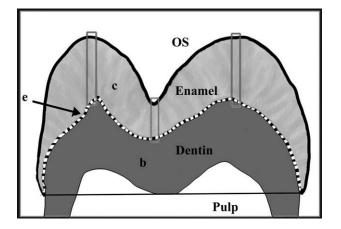

Fig. 2. Schematic of the cross-section of a tooth with enamel, dentin, pulp, occlusal surface (OS), and enamel dentin junction (EDJ) (e) labeled. Gray rectangles indicate the approximate location of indentation test arrays placed on each tooth. Additionally, this image shows the measurements recorded in this study used to calculate the RET: c the cross-sectional area of the enamel cap, b the cross-sectional area of the dentin enclosed by enamel cap, and e the length of the EDJ.

substantially thicker enamel, yet still required 28–44 rows of indents to cover the complete area from EDJ to OS.

To further understand the variation in mechanical properties, each nanoindentation array was spatially divided into halves, the half of enamel thickness adjacent to the OS and the half adjacent to the EDJ, based on the percent distance of the enamel thickness at each array location. Data were taken from the EDJ half permitted comparison of properties between species from unworn and undamaged enamel.

Quantitative backscatter electron imaging

Quantitative backscatter electron (qBSE) imaging was used to analyze the relative mineral content of each indentation location and enabled examination of tooth microstructure and microcracking. Following nanoindentation testing, the PMMA-embedded teeth were coated with carbon, and each indentation array was imaged using an SEM with backscatter detector (JEOL 6480LV) operated at 20 kV with a 15-mm working distance and a spot size of 60. Gray-level images, with pixel values ranging from of zero for black to 255 for white, of each indentation array were taken at 500× after an hour of SEM warm up time to insure stabilized conditions. The gray-level value of an individual pixel is dependent on the number of measured backscattered electrons, which is directly related to the mean atomic number of the
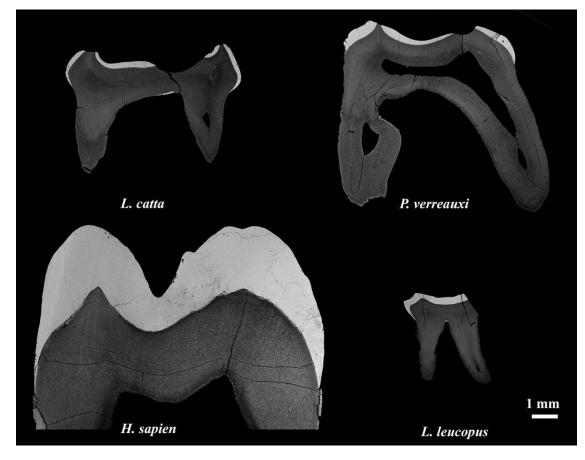

Fig. 3. Compilations of backscattered electron images of the cross-section of a molar for each species: *L. leucopus*, *P. verreauxi*, *L. catta*, and *H. sapiens*. Images were taken in backscatter mode at 20 kV, with 15 mm working distance, and a spot size of 60. Clear wear patterns are present on *L. catta* and *P. verreauxi*.
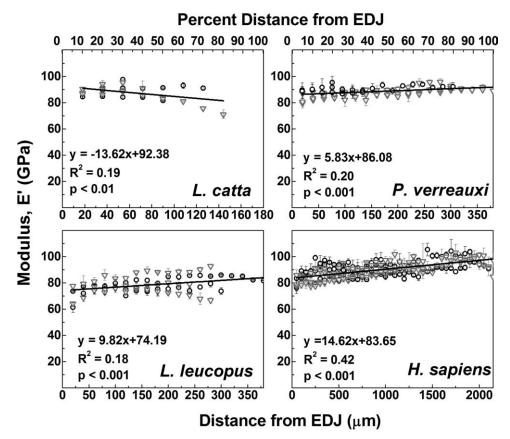
Percent Distance from EDJ

Fig. 4. Nanoindentation modulus of three lemur species and human dental enamel. Open circles and closed triangles each represent an individual sample. Three indentation arrays were placed on each sample perpendicular to and covering the area from EDJ to the OS. Each data point represents the mean ± standard deviation of four (three for human sample) indentations taken in a row at equal distance from the EDJ (distance = 0) to the OS. Rows were spaced at 20 μm in lemur and 50 μm in human samples. Linear fit equation for all data points is listed.

sample at that location (Lloyd, 1987; Howell et al., 1998). To permit comparison between imaging sessions, novel lithium–rubidium borosilicate glass standards of the composition $(0.25 - x)$ $Li_2O \cdot$ $xRb_2O \cdot$ $0.30B_2O \cdot$ $0.45SiO_2$ (with $x = 0.05$ and 0.15) were imaged at the start, every 10 min, and again at the end of each imaging session. The histogram for each image of enamel was stretched over the 256 gray levels where the measured gray level of the glass standard $x = 0.05$ was set to zero and $x = 0.15$ was set to 255 to encompass the range of gray scale values of enamel. Similar methods of qBSE analysis have been used often with the use of polymeric and metallic materials (Boyde and Jones, 1983; Skedros et al., 1993; Boyde et al., 1995; Vajda et al., 1995).

Site-matched measurements of qBSE-weighted mean gray level (WMGL) were performed within a circle around each nanoindentation site. The WMGL is the average of gray-level values from each pixel within the region of interest. The effective volume of material contributing to the overall mechanical response depends on factors that include the indenter contact depth and the size of the tip and can be described by a paraboloid of revolution with radius $3a$ and depth $5a$ (where a = radius of circle of contact between the tip and the surface) (Ferguson et al., 2003). The contact radius, a, was calculated from the calibrated tip area function (A_c) assuming a circular contact at the maximum depth of contact

($\approx$800 nm). WMGL was measured within a circular region (radius = $3a$ or 6 μm) around each indentation site (see Fig. 1A). Using NIH Image J (U.S.A. National Institutes of Health, Bethesda, MD), the residual indentation imprint, cracks, and any other void spaces were removed from analysis though a threshold routine (Campbell, 2010).

Cracking analysis

Analysis of nanoindentation tests taken near microcracks, and not included in the primary data set, allows for quantitative measurements of damaged regions of enamel. Backscattered electron images of each indentation array were used to bin each indent location into four cracking classifications based on the distance of the test site to the nearest crack: Category 1 = ideal indent location with no visible damage, Category 2 = indent site is >1 and ≤3 indent widths from a crack, Category 3 = indent site is ≤1 indent width from a crack, and Category 4 = indent is directly on a crack or visible damage. Figure 1A demonstrates the categories assigned to indents in an example array. All analyses only include category 1 or ideal indent locations except where specifically stated to include categories 2–4. The extent of cracking in each sample was defined as the number of indentation sites within three indent-widths of a crack (the sum of groups 2, 3, and 4) divided by the total num-
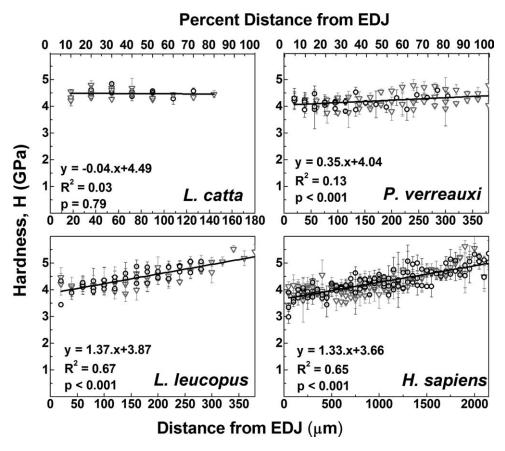
Fig. 5. Nanoindentation hardness of dental enamel of three lemur species plus humans. Open circles and closed triangles each represent an individual sample. Three indentation arrays were placed on each sample perpendicular to and covering the area from the EDJ to the occlusal surface. Each data point represents the mean ± standard deviation of four (three for humans) indentations taken in a row at equal distance from the EDJ (distance = 0) to the OS. Rows were spaced at 20 μm in lemurs and 50 μm in human samples. Linear fit equations for all data points are listed.

ber of indentation sites ×100%. It should be noted that cracking was present in the majority of samples near the EDJ. The authors have commonly observed similar cracking artifacts as the result of dehydration. To remove these artifacts from our analysis, all data points near an EDJ crack have been removed from both cracking and primary analysis sets.

Backscatter electron images of the cross-section of each sample were used to measure the enamel thickness (see Fig. 3) using Image J. The measurement of the relative enamel thickness (RET), a dimensionless index, allows for comparison of enamel thickness independent of the size of the tooth (Martin, 1985). Calculation of the RET is given by the area of the enamel cap (c) divided by the length of the EDJ (e) and then divided by the square root of the area of the dentin (b) multiplied by 100. For each sample, the lengths and areas (c, e, and b) were measured (see Fig. 2) three times and averaged to reduce measurement error. Differences in measured values were minimal as the mean coefficient of variance (COV) was 1.8%. Although RET measurements are generally made on unworn samples, measurement on our samples allowed for a quantitative assessment of gross wear. The *L. leucopus* sample 2 was fractured and missing a portion of the tooth (see Fig. 3); therefore, RET measurements were made using only half the tooth to the midline and doubled; nevertheless, this produced a result similar to that of *L. leucopus* sample 1. Measure-

ments made on worn teeth are called worn-RET values hereafter and can be used to quantify the amount of wear when compared with non-worn RET values from the literature.

After all other analyses, one sample from each species was etched to allow visualization of microstructure following the method of Boyde et al. (1978) using 0.5% H_3PO_4 for 60 s and then coated with a conductive carbon coating. Samples were reimaged using secondary electron (SE) imaging with a JEOL 6480LV SEM operated at 10 kV with an 18-mm working distance and a spot size of 30. SE images were used to determine prism pattern and orientation at the EDJ and OS of one representative sample from each species. Average prism width for each species was measured near the OS on 10 randomly selected prisms from an SEM image taken near the cusps of each sample.

RESULTS
Nanomechanical measurements

Nanomechanical property trends were similar in all species, except *L. catta*, where E' and H values significantly increased ($P < 0.001$) from the EDJ toward the OS. Alternatively, *L. catta* showed decreased modulus values and unchanging hardness values (Figs. 4 and 5). Similarly, the modulus and hardness values from the

TABLE 3. *Indentation modulus and hardness values are presented along with qBSE data for all lemur species and human enamel*

Sample	H (GPa), EDJ half	H (GPa), OS half	H %Δ	E' (GPa), EDJ half	E' (GPa), OS half	E' %Δ	WMGL, EDJ half	WMGL, OS half	WMGL %Δ
H. sapiens 1	4.05 ± 0.25 (143)	4.58 ± 0.47 (155)	12.40[a]	91.12 ± 3.76 (143)	97.43 ± 4.90 (155)	6.70[a]	170.45 ± 3.72 (143)	173.19 ± 5.20 (155)	1.59[a]
H. sapiens 2	4.04 ± 0.29 (133)	4.60 ± 0.45 (155)	12.97[a]	86.34 ± 4.59 (133)	94.82 ± 4.70 (155)	9.36[a]	167.79 ± 3.18 (133)	170.35 ± 4.08 (155)	1.51[a]
Mean of *H. sapiens*	4.04 ± 0.00 (2)	4.59 ± 0.02 (2)	12.68	88.73 ± 3.38 (2)	96.13 ± 1.85 (2)	8.00	169.12 ± 1.88 (2)	171.77 ± 2.01 (2)	1.86
P. verreauxi 1	4.12 ± 0.27 (44)	4.39 ± 0.34 (84)	6.39[a]	86.00 ± 3.02 (44)	90.55 ± 2.72 (80)	5.15[a]	173.48 ± 4.18 (44)	174.80 ± 2.95 (84)	0.76
P. verreauxi 2	4.13 ± 0.29 (30)	4.21 ± 0.30 (57)	1.99	88.89 ± 3.72 (30)	89.96 ± 4.59 (57)	1.23	169.23 ± 1.44 (30)	170.10 ± 1.30 (57)	0.53
Mean of *P. verreauxi*	4.13 ± 0.01 (2)	4.30 ± 0.13 (2)	4.21	87.44 ± 2.04 (2)	90.23 ± 0.39 (2)	3.18	171.87 ± 2.91 (2)	172.20 ± 2.46 (2)	0.64
L. catta 1	4.42 ± 0.18 (25)	4.55 ± 0.25 (21)	2.81	87.95 ± 2.40 (25)	86.32 ± 9.02 (21)	−1.87	168.18 ± 9.16 (25)	171.57 ± 8.76 (21)	2.00
L. catta 2	4.43 ± 0.19 (22)	4.52 ± 0.71 (24)	2.03	88.59 ± 3.18 (22)	87.93 ± 5.03 (24)	−0.75	170.43 ± 5.14 (22)	170.86 ± 4.25 (24)	0.25
Mean of *L. catta*	4.43 ± 0.00 (2)	4.54 ± 0.17 (2)	2.42	88.27 ± 0.45 (2)	87.12 ± 1.14 (2)	−1.31	169.31 ± 1.59 (2)	171.22 ± 0.50 (2)	1.12
L. leucopus 1	4.30 ± 0.32 (58)	4.83 ± 0.56 (90)	11.77[a]	77.88 ± 4.91 (58)	79.33 ± 5.38 (90)	1.84	168.56 ± 1.94 (58)	170.33 ± 2.49 (90)	1.66[a]
L. leucopus 2	4.20 ± 0.30 (36)	4.63 ± 0.32 (77)	9.84[a]	78.48 ± 4.91 (36)	79.34 ± 7.69 (77)	1.08	170.29 ± 7.09 (36)	173.78 ± 7.98 (77)	2.03[a]
Mean of *L. leucopus*	4.25 ± 0.07 (2)	4.73 ± 0.14 (2)	10.82	78.18 ± 0.42 (2)	79.33 ± 0.00 (2)	1.41	169.43 ± 1.22 (2)	172.06 ± 2.43 (2)	1.54

Data were divided into two groups for each species for comparison near the EDJ or OS. For each of these groups, data are presented as the mean ± standard deviation (*n*-value). Additionally, the difference between the EDJ and OS was determined as [%Δ = (OS − EDJ)/((EDJ + OS)/2) × 100].
[a] Indicates statically significant p < 0.05 using a Student's *t*-test.

OS-half were 1.08–12.97% greater than that of the EDJ-half (significance shown in Table 3) for all species except *L. catta*. Comparison of the unworn enamel within the EDJ-half demonstrated little species variation, as the mean modulus was 88.15 ± 0.65 GPa for all of the species except *L. leucopus*, which had a mean modulus of 78.18 ± 0.42 GPa (Table 3). Yet, variations of mechanical properties between species were evident in the mechanical properties of the OS-half. The mean moduli of *L. catta*, *P. verreauxi*, and *L. leucopus* were reduced compared to human enamel by 6.1, 9.4, and 17.5%, respectively (Table 3).

Mineralization and microstructural variations

Figure 3 contains SEM images of the whole enamel surface for one sample of each species investigated. Severe wear was clearly visible on both *L. catta* and *P. verreauxi* M² teeth. Minor amounts of wear were evident on *L. leucopus* sample 1 and *P. verreauxi* sample 1 (not pictured), and the remaining samples had little evidence of wear. Measurements of worn-RET listed in Table 2 clearly reflect the severe wear present on both *L. catta* samples and *P. verreauxi* sample 2 with reduced values compared to those reported previously in the literature (Godfrey et al., 2005).

qBSE-imaging WMGL, a relative measure of mineral content, was calculated for each indentation point and grouped into OS and EDJ halves (Table 3). WMGL slightly increased from the EDJ to the OS with a mean increase of 1.3% for all species (Table 3). Yet significant increases in WMGL were only observed in humans and *L. leucopus*, the two species that displayed little to no wear.

Additionally, prism orientation varied from the EDJ with more randomly oriented prisms with Hunter–Schreger bands (HSB) to radially oriented prisms at the OS for all samples except *L. leucopus* (see Fig. 6). There was no evidence of HSB in the *L. leucopus* samples. Both prism patterns and prism width observed in each species are reported in Table 2. Prism width scaled with the mass of the species as human enamel had the widest prisms, and *L. leucopus*, the lightest species, had a 48% reduction in prism width compared to humans. Prism widths were similar to those previously reported ranging from 3.5 to 6 μm for a variety of lemur species (Maas, 1994).

Detection of microdamage with nanoindentation

Nanoindentation test sites within one indent width of a crack (categories 3 and 4) had increased depth of penetration or plastic deformation in load-displacement curves (Fig. 1B). Furthermore, indentation testing within three indent widths of the testing site (categories 2–4) resulted in reduced modulus and hardness values reported in Table 5 as grouped by species. For all species, there was an average decrease in modulus of 5% and hardness of 7% from category 1 to 2. Further reductions in mechanical properties were observed with decreased distance from the indent site to a crack. For example, in group 4, an average 44% decrease in modulus and 58% decreases in hardness were observed compared to group 1.

Microcracks were visible on all samples and were primarily located near the EDJ except in *L. catta* (Figs. 1 and 7) where substantial cracking was also visible at the OS (Table 4). Microcracks near the EDJ are likely the
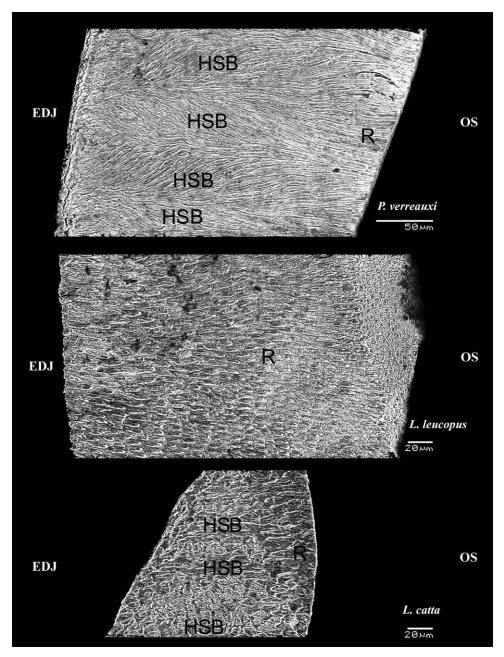
Fig. 6. Secondary electron images taken at 10 kV of etched enamel for one sample from each lemur species. HSB are present in all species except *L. leucopus*, which has only radially (R) oriented prism. Radially (R) oriented prisms were also present at the OS of all species.

result of dehydration as authors have previously observed similar cracking in laboratory controlled dehydration processes. In *L. catta*, 43% of all test locations landed within three indent-widths of a crack (categories 2–4) compared to an average of only 14% of testing sites on the other samples. Additionally, microcracks on *L. catta* were located at a distance of 73% of the enamel thickness from the EDJ compared to an average distance of 49% of the enamel distance in the other species.

DISCUSSION

The complex functionality of primate teeth depends on mechanical and material characteristics as well as other properties including size, shape, and enamel thickness (Gregory, 1922; Crompton and Sita-Lumsden, 1970; Kay and Hiiemae, 1974; Maas and Dumont, 1999). Although whole tooth morphology has been widely characterized in studies of primate diet and microwear [see reviews in Ungar (1998, 2002) and Teaford (2000a)], investigation of mechanical properties has been limited (Constantino et al., 2009; Darnell et al., 2010; Lee et al., 2010). In this study, variations in enamel microstructure, mineralization, and mechanical properties were explored within single molars and between lemur species and humans. Comparison of enamel at the EDJ revealed similar mean properties between species except *L. leucopus*. However, significant intratooth variability was evident as the COV

within each sample ranged from 4.0 to 11.9% for H and E', indicating the heterogeneity of enamel that is inherently linked to variations in mineralization and microstructural properties.

Property variations between species

Our reported mean E' and H values fit within the range of values in mammalian enamel previously measured by nanoindentation (Table 1). Furthermore, our human data corresponds with previous studies of the nanomechanical properties of human enamel (Habelitz et al., 2001; Cuy et al., 2002; Zhou and Hsiung, 2007) (Tables 1 and 3). Although variations in the mechanical properties of the teeth of several species have been reported, meaningful comparison is difficult as these studies have low n-values and often only report a mean value for an entire tooth. As shown here and elsewhere, large variations in mechanical properties exist from the EDJ to the OS in primate enamel (Constantino et al., submitted; Cuy et al., 2002; Darnell et al., 2010), indicating that average mechanical values are not representative and are not an ideal way to compare species. Additionally, large variation in mechanical properties exists between different teeth within one animal (i.e., M^1 vs. M^3, see Table 1) (Darnell et al., 2010). An alternative comparison of mechanical properties between species might be made through values near the EDJ (Table 3), especially when considering samples that have been worn by mastication. In this study, comparison of the moduli near the EDJ demonstrated little variation

TABLE 4. Data from the two samples within each species were grouped to determine the percent cracking and location based on the percent distance from the enamel dentin junction

Species	% cracking	% distance
L. catta	43.2	73.2
P. verreauxi	22.1	46.6
L. leucopus	16.6	38.4
H. sapiens	2.5	60.5

The % cracking was calculated as the sum of all indents within three indent widths or less of a crack (categories 2, 3, and 4) divided by the total number of indent sites [(category 2 + 3 + 4)/(total no. of indents)]. Percent distance (% distance) is calculated as the location of the indent divided by the total distance from the EDJ to OS for each array.

between samples, as the modulus was similar for all of the species except *L. leucopus*. Recently, Darnell et al. (2010) proposed a similar method of comparison between samples and reported *Alouatta palliata* (howler monkey) buccal cusp modulus values near the EDJ to have modulus values of 85 and 77 GPa for M^3 and M^1, respectively. Although these values are in the range of our measured values, a direct comparison is difficult as we sampled M^2 and large variations in mechanical properties clearly exist between different molars (Darnell et al., 2010).

Mechanical property gradient

In addition to a mean value for E' and H, the gradient in mechanical values from the EDJ to OS needs to be considered when comparing species. There was a general increase in mechanical properties from the EDJ to the

TABLE 5. Nanoindentation data were classified into 4 groups based on location of indent test site to a micro crack

Crack category (n)	$H \pm$ SD (GPa)	$E' \pm$ SD (GPa)
H. sapien 1 (578)	4.34 ± 0.48[*,**]	92.73 ± 6.14[*,**,***]
2 (9)	3.99 ± 0.57	85.22 ± 3.04
3 (4)	4.08 ± 0.12	83.44 ± 1.39
4 (2)	0.93 ± 1.13	37.12 ± 31.30
P. verreauxi 1 (215)	4.26 ± 0.33[***]	89.54 ± 3.98[**,†]
2 (28)	3.97 ± 0.29	85.58 ± 3.14
3 (24)	3.92 ± 0.22	83.85 ± 2.49
4 (8)	2.07 ± 1.04	60.23 ± 15.26
L. catta 1 (92)	4.48 ± 0.21[***,†]	87.73 ± 5.36[**,†]
2 (13)	4.43 ± 0.27	86.23 ± 7.95
3 (25)	3.88 ± 0.62	76.07 ± 14.16
4 (32)	2.53 ± 1.53	54.12 ± 28.08
L. leucopus 1 (261)	4.57 ± 0.48[***,†]	78.89 ± 5.87[*,***,†]
2 (13)	4.09 ± 0.70	75.97 ± 10.97
3 (32)	3.98 ± 0.36	71.21 ± 5.55
4 (7)	2.00 ± 1.83	42.74 ± 22.41

Categories represent: 1 = perfect indent location with no visible damage, 2 = crack distance greater than one to three indent widths away from indent location, 3 = crack located within one indent width for test site, and 4 = indent on top of crack or visible damage. One-way ANOVA with a Bonferroni follow on test was used to compare difference between species on grouped data from the two samples with category 1 data. Significant differences between groups indicated for $P < 0.05$ where * = versus *H. sapien*, ** = versus *P. verreauxi*, *** = versus *L. catta*, † = versus *L. leucopus*.
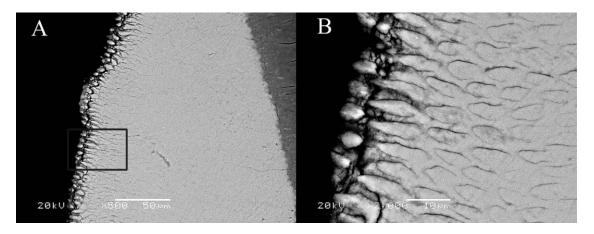

Fig. 7. BSE image of *L. catta* sample 1 demonstrating extreme cracking present at the OS. Images taken of non-etched enamel at 20 kV with a 15-mm working distance. Image **B** gives an enlarged view of the boxed region in image **A**.

OS in modulus and hardness for all species except *L. catta* (Figs. 4 and 5). The difference seen in *L. catta* is unexpected and is likely the result of the extreme cracking present at the OS (further discussed later). A similar gradation in mechanical properties toward the OS has been observed in many primates (Constantino et al., submitted; Cuy et al., 2002; He and Swain, 2009; Darnell et al., 2010; Lee et al., 2010). Gradation of mechanical properties may help transmit load into the supporting dentin and possibly prevent crack formation. The steepness of the gradation of nanomechanical properties is variable between the species as demonstrated by the percent difference in E' and H between the EDJ and OS half (Table 3). *H. sapiens* displayed the largest gradient of mechanical properties with 12.7% increases in hardness and an 8% increase in modulus from the EDJ to OS. Lemur species had smaller differences in intratooth mechanical properties, which may be linked to thinner enamel or wear of the outer surface. The large mechanical property increases and associated higher values of modulus and hardness are likely one advantage of possessing thicker enamel. Both *L. catta* samples and *P. verreauxi* sample 2 had the most measurable wear and the smallest increase in mechanical properties, suggesting that the hardest outer portion of the enamel surface had been removed though the wear process. This is not a surprise, given the wear that occurs in these two species at Beza Mahafaly, especially the dramatic wear seen in ring-tailed lemurs, which far exceeds that in Verreaux's sifaka (e.g., Cuozzo and Sauther, 2006, Cuozzo et al., 2008).

A general trend of increasing WMGL was present from the EDJ to the OS, which corresponds with the increase in mechanical properties in all species except *L. catta*. The human molars had the largest increase in WMGL, which corresponded with the largest increase in mechanical properties (Table 3). Our findings corroborate previous results, which correlated increased mechanical properties to increased mineral content (Robinson et al., 1995; Cuy et al., 2002; Angker et al., 2004). In human enamel, weight percent mineral has shown to increase from 84% at the EDJ to 96% at the OS (Robinson et al., 1995). Variations in mineral density have also been observed in *Alouatta palliata* (howler monkey) enamel where mineral content (P_2O_5 and CaO) was highest at the hard OS and decreased toward the EDJ, corresponding with mechanical properties (Darnell et al., 2010).

Mineralization and microstructure

Although increased mineralization can account for general E' and H increases from the EDJ to the OS, the difference in WMGL between species was minimal and cannot explain the lower modulus values in *L. leucopus*. The microstructure of enamel is also known to contribute to the measured mechanical properties through prism orientation (Spears, 1997; Jiang et al., 2005) and prism size (He et al., 2006). Prism orientation in all species except *L. leucopus* was randomly oriented near the EDJ with the presence of HSB and radially oriented at the OS. It has been suggested that the majority of primates with a body mass less than 2000 g generally do not display HSB (Maas and Dumont, 1999) and *L. leucopus* is no exception. HSB are thought to help stop crack propagation and may provide increased toughness to the whole tooth. The layer of radially oriented prisms at the OS might act as a stiff functional surface for

mastication as anisotropic enamel prisms have higher mechanical properties in the axial direction than longitudinal direction (Spears, 1997; Jiang et al., 2005). As this functional layer is worn away, more randomly oriented prisms are revealed, which are less stiff and may be prone to higher rates of wear. In this study, no mechanical property variations were attributed to prism orientation as all prisms were tested in the primarily transverse direction. A similar conclusion was reached using nanoindentation of human molars (Braly et al., 2007). Nanoindentation is a multiaxial test (averaging properties in x, y, and z) and therefore less sensitive to anisotropy and small changes of prism orientation as created by HSB. Further, our data were averaged over three to four indentation points with variable prism orientations, effectively averaging out the effect of anisotropy in the underlying tissue.

Variation in prism size may have resulted in *L. leucopus*'s reduced modulus values. Recently, using AFM-based nanoindentation, Ge et al. (2005) have reported that the modulus and hardness of the prism sheaths were about 73.6% and 52.7% lower than those of the prisms. In indentation testing, the volume of deformed material increases with the depth of penetration of the indenter tip (Johnson, 1985). Thus, a low depth indent (similar to those reported with AFM indentation) when placed at the center of a prism will test only the crystals within that single prism. As the depth of the indent increases, a larger volume may include both prisms and sheath, and the resultant mechanical properties will be reduced compared to a test that only samples the material within the prism. This concept has been demonstrated in human enamel where mechanical properties decrease with an increasing indentation depth and thus also increasing contact radius (a) (He et al., 2006; Zhou and Hsiung, 2007). In the current study, an indentation depth of about 800 nm results in $a = 2.2$ μm or diameter of 4.4 μm. Every randomly placed indentation site likely mechanically tests the combined properties of the prisms and surrounding sheaths. For *H. sapiens* with the largest average prism diameter (6.3 μm), there is a chance that an indent may fall directly in the center of a prism and test primarily the prism's and not the sheath's mechanical properties. However, for *L. leucopus*, with the smallest prism diameter ($\sim$3.8 μm), every test volume included sheath material potentially explaining *L. leucopus*'s reduced modulus values. Furthermore, AFM indentation showed the sheath to experience a larger decrease in modulus than hardness values compared to the prism (Ge et al., 2005), which may indicate a potential mechanism for reduced modulus, but not hardness, values in *L. leucopus*.

Lemur catta microcracking and wear

L. catta displayed substantial wear in both samples as evident from worn-RET compared to literature RET values (Table 2). Furthermore, *L. catta* had substantial cracking compared to other species (Table 4). The Beza Mahafaly *L. catta* population have been shown to exhibit extreme tooth wear and antemortem tooth loss as a result of processing a mechanically challenging fallback food (tamarind fruit) with their extremely thin enamel (Sauther et al., 2002; Cuozzo and Sauther, 2004; Cuozzo and Sauther, 2006; Sauther and Cuozzo, 2009). Yamashita et al. (this volume) directly measured the mechanical properties of individual food parts in

the diet *L. catta* over 4 different years. The tamarind fruit is the toughest and hardest food ingested by *L. catta* and the most frequently eaten by volume. Furthermore, the tamarind fruit shell was observed to require high and repeated loads to crack (Yamashita et al., this volume).

It has been suggested that frequently consumed fall-back foods, such as the tamarind fruit, contribute rapidly to alterations of dentition (Kinzey, 1987; Yamashita, 1998; Lambert et al., 2004; Cuozzo and Sauther, 2006, 2009). Because the morphology of *L. catta* molars indicates an adaptation to folivory (Seligsohn, 1977; Yamashita, 1998), dependence on tamarind fruit in these gallery forests of southern Madagascar likely has only recently occurred. Our study supports this finding, as *L. catta*'s enamel mechanical properties are most similar to *P. verreauxi*, a more dedicated folivore, with dental morphology clearly adapted for a diet dominated by leaves (e.g., Yamashita, 1998; Cuozzo and Sauther, 2006; Cuozzo et al., 2008). *P. verreauxi*'s dietary toughness is not significantly different from that of *L. catta* (Yamashita, 2008). Furthermore, *P. verreauxi* has been observed to consume the tamarind fruit at Beza Mahafaly, although they typically consume the seeds from the unripe fruit (Yamashita, 2008). The unripe fruit has been shown to be less tough than the ripe fruit, which may contribute to the wear observed in *L. catta* (Yamashita et al., submitted). Given the similarity in these species' enamel and average diet toughness, it is likely that *L. catta*'s tooth morphology (e.g., thin enamel) along with consumption of the ripe tamarind fruit is the primary culprits for the observed tooth wear and antemortem tooth loss at Beza Mahafaly.

Notable cracking present in the OS half (Table 4 and Fig. 7) corresponds to significantly reduced modulus and hardness values (Table 5) of the *L. catta* samples in this study and further points to the extreme wear and damage caused by the consumption of the tamarind fruit. It should be noted that all lemur tooth samples were collected under similar conditions (i.e., from the forest floor at Beza Mahafaly). The human samples were dehydrated in laboratory-controlled conditions though a series of ethanol solutions, yet displayed similar cracking trends to *L. leucopus* and *P. verreauxi* with cracking along the EDJ. These similarities emphasize that the unknown dehydration conditions in Beza Mahafaly are secondary, and the substantial cracking present near the OS in *L. catta* (as depicted in Figs. 1 and 7) is unlikely to be the result of dehydration conditions. There was no change in WMGL within the cracked region indicating that reduced mechanical properties are not the result of demineralization from the acidic tamarind fruit, but were more likely a result of mechanical abrasion. Data on the potential buffering capacity of lemur saliva, which likely mitigates tooth erosions from acidic tamarind fruit (Cuozzo et al., 2008), provide further support for this assertion.

Cracking in enamel is a cumulative process as no remodeling of the tissue occurs over the lifetime of the animal. The process of cracking likely accelerates the rate of wear as reduced mechanical properties were evident in *L. catta* at test sites away from visible microcracks (see Fig. 1). It is likely that subsurface cracking contributed to the reduced modulus values near the OS. Furthermore, nanoindentation provides a novel tool that may be used to detect such non-visible damage within mammalian enamel.

These data have broad implications for interpreting ecology through an organism's teeth. It is well known that enamel thickness and organization (e.g., enamel decussation) correlate with diet, ecology, and behavior, although the exact relationships can, at times, be somewhat messy (e.g., Martin et al., 2003). Among the recently extinct fossil lemurs of Madagascar, enamel thickness and organization have been used to extrapolate the diet of the animals (e.g., Godfrey et al., 2005). For example, the thick enamel and complex decussation in the extinct archaeolemurids (e.g., *Archaeolemur* and *Hadropithecus*) have been linked to specific diets (e.g., Godfrey et al., 2005). Our data suggest that the mechanical properties of extant lemurs can inform questions related to diet among the extinct forms, if assessed using nanoindentation methods. This method transcends lemurs and can be applied to other extinct primates. One example is *Cercopitehcoides kimeui*, which displays a pattern of severe tooth wear at the end of the Pliocene, thought to be related to the shifting ecology of East Africa approaching the Plio-Pleistocene transition (Jablonski and Leakey, 2008). Collection of nanoindentation data from this species, when compared with sympatric, related forms, which did not become extinct, could elucidate "weaknesses" in the enamel structure of this species, which may explain the inability of this primate to adjust to a rapidly changing environment. This one example illustrates the potential for nanoindentation data to inform questions about primate paleobiology.

CONCLUSION

A complete understanding of functional adaptations of the tooth requires knowledge of the microstructure, mineralization, and nanomechanical properties of enamel in addition to the more commonly investigated morphology and enamel thickness. Our data on nanomechanical properties across three sympatric lemur species illustrates an overall similarity in their enamel structure with similar property trends increasing from the EDJ to the OS. Variations in mechanical properties were linked to changes in mineral content and microstructure. The different patterns of dental wear and tooth damage seen in these three species, despite their similar enamel properties as we describe herein, indicate that ring-tailed lemurs are not well-suited to consumption of their fall-back food, the tamarind fruit. As all extant (and extinct lemurs) belong to a monophyletic group, with a single origin early in the Tertiary, it is not surprising that each of these three species would share certain enamel properties. However, when combined with patterns of tooth wear, dental morphology, and feeding ecology, nanoindentation analysis provides a new tool with which to assess and understand primate "dental ecology."

ACKNOWLEDGMENTS

LITERATURE CITED

Angker L, Nockolds C, Swain MV, Kilpatrick N. 2004. Quantitative analysis of the mineral content of sound and carious primary dentine using BSE imaging. Arch Oral Biol 49:99–107.

Boyde A, Davy K, Jones S. 1995. Standards for mineral quantitation of human bone by analysis of backscattered electron images. Scanning 17:6–7.

Boyde A, Jones SJ. 1983. Back-scattered electron imaging of skeletal tissues. Metab Bone Dis Relat 5:145–150.

Boyde A, Jones SJ, Reynolds PS. 1978. Quantitative and qualitative studies of enamel etching with acid and EDTA. In: Becker RP, Johari O, editors. Scanning electron microscopy. Chicago: SEM Inc. pp 991–1002.

Boyde A, Martin L. 1982. Enamel microstructure determination in hominoid and cercopithecoid primates. Anat Embryol 165:193–212.

Braly A, Darnell LA, Mann AB, Teaford MF, Weihs TP. 2007. The effect of prism orientation on the indentation testing of human molar enamel. Arch Oral Biol 52:856–860.

Campbell SE. 2010. Nanoindentation of bio- and geo-mineralized composites: contribution of microstructure and composition, PhD Thesis, University of Colorado, Boulder, CO.

Crompton AW, Sita-Lumsden A. 1970. Functional significance of therian molar pattern. Nature 227:197.

Cuozzo F, Sauther ML. 2004. Tooth loss, survival, and resource use in wild ring-tailed lemurs (*Lemur catta*): implications for inferring conspecific care in fossil hominids. J Hum Evol 46:623–631.

Cuozzo FP, Sauther ML. 2006. Severe wear and tooth loss in wild ring-tailed lemurs (*Lemur catta*): a function of feeding ecology, dental structure, and individual life history. J Hum Evol 51:490–505.

Cuozzo FP, Sauther ML, Yamashita N, Lawler RR, Brockman DK, Godfrey LR, Gould L, Youssouf IAJ, Lent C, Ratsirarson J, Richard AF, Scott JR, Sussman RW, Villers LM, Weber MA, Willis G. 2008. A comparison of salivary pH in sympatric wild lemurs (*Lemur catta* and *Propithecus verreauxi*) at Beza Mahafaly Special Reserve, Madagascar. Am J Primatol 70:363–371.

Cuy JL, Mann AB, Livi KJ, Teaford MF, Weihs TP. 2002. Nanoindentation mapping of the mechanical properties of human molar tooth enamel. Arch Oral Biol 47:281–291.

Darnell L, Teaford M, Livi K, Weihs T. 2010. Variations in the mechanical properties of *Alouatta palliata* molar enamel. Am J Phys Anthropol 141:7–15.

Dumont ER. 1995. Enamel thickness and dietary adaptation among extant primates and chiropterans. J Mammal 76:1127–1136.

Feng G, Ngan AHW. 2002. Effects of creep and thermal drift on modulus measurement using depth-sensing indentation. J Mater Res 17:660–668.

Ferguson VL. 2004. Elastic modulus of dental enamel: effect of enamel prism orientation and mineral content. Mater Res Soc Symp Proc 841:R2.7–Y2.7.

Ferguson VL, Bushby AJ, Boyde A. 2003. Nanomechanical properties and mineral concentration in articular calcified cartilage and subchondral bone. J Anat 203:191–202.

Ferguson VL, Olesiak SE. 2010. Nanoindentation of bone. In: Oyen ML, editor. The handbook of nanoindentation with biological applications. Singapore: Pan Stanford.

Fleagle J. 1998. Primate adaptation and evolution. New York: Academic Press.

Forbes HO. 1894. A handbook to the primates. London: WH Allen Co.

Ge J, Cui F, Wang X, Feng H. 2005. Property variations in the prism and the organic sheath within enamel by nanoindentation. Biomaterials 26:3333–3339.

Godfrey LR, Semprebon GM, Schwartz GT, Burney DA, Jungers WL, Flanagan EK, Cuozzo FP, King SJ. 2005. New insights into old lemurs: the trophic adaptations of the Archaeolemuridae. Int J Primatol 26:825–854.

Gregory WK. 1922. The origin and evolution of the human dentition. Baltimore: Williams & Wilkins.

Habelitz S, Marshall SJ, Marshall GW, Balooch M. 2001. Mechanical properties of human dental enamel on the nanometre scale. Arch Oral Biol 46:173–183.

Harcourt C, Thornback J. 1990. Lemurs of Madagascar and the Comoros. The IUCN Red Data Book. Cambridge, UK: ICUN Gland.

He LH, Fujisawa N, Swain MV. 2006. Elastic modulus and stress-strain response of human enamel by nano-indentation. Biomaterials 27:4388–4398.

He LH, Swain MV. 2008. Understanding the mechanical behaviour of human enamel from its structural and compositional characteristics. J Mech Behav Biomed 1:18–29.

He LH, Swain MV. 2009. Enamel—a functionally graded natural coating. J Dent 37:596–603.

Hill WCO. 1954. Primates. Comparative anatomy and taxonomy. Edinburgh: Edinburgh University Press.

Howell PGT, Davy KMW, Boyde A. 1998. Mean atomic number and backscattered electron coefficient calculations for some materials with low mean atomic number. Scanning 20:35–40.

Jablonski NG, Leakey GL. 2008. The fossil monkeys. San Francisco: California Academy of Sciences.

Jiang HD, Liu XY, Lim CT, Hsu CY. 2005. Ordering of self-assembled nanobiominerals in correlation to mechanical properties of hard tissues. Appl Phys Lett 86:163901.

Johnson KL. 1985. Contact mechanics. Cambridge, UK: Cambridge University Press.

Jolly A. 1967. Lemur behavior. Chicago: University of Chicago Press.

Jolly A, Koyama N, Rasamimanana H, Sussman RW. 2006. Ringtailed lemur biology: *Lemur catta* in Madagascar. Boston: Springer.

Kay RF. 1975. Functional adaptations of primate molar teeth. Am J Phys Anthropol 43:195–215.

Kay RF. 1981. The nut-crackers—a new theory of the adaptations of the Ramapithecinae. Am J Phys Anthropol 55:141–151.

Kay RF, Hiiemae KM. 1974. Jaw movement and tooth use in recent and fossil primates. Am J Phys Anthropol 40:227–256.

Kinzey WG. 1987. Comparative functional-morphology of the dentition of bearded saki and spider monkeys. Anat Rec 218:A72–A72.

Lambert JE, Chapman CA, Wrangham RW, Conklin-Brittain NL. 2004. Hardness of cercopithecine foods: implications for the critical function of enamel thickness in exploiting fallback foods. Am J Phys Anthropol 125:363–368.

Lebel S, Trinkaus E. 2002. Middle Pleistocene human remains from the Bau de l'Aubesier. J Hum Evol 43:659–685.

Lee JW, Morris D, Constantino P, Lucas P, Smith TM, Lawn BR. 2010. Properties of tooth enamel in great apes. Acta Biomater 6:4560–4565.

Lloyd G. 1987. Atomic-number and crystallographic contrast images with the SEM—a review of backscattered electron techniques. Mineral Mag 51:3–19.

Lucas P. 2004. How teeth work. Cambridge, UK: Cambridge University Press.

Lucas P, Constantino P, Wood B, Lawn B. 2008. Dental enamel as a dietary indicator in mammals. Bioessays 30:374–385.

Maas MC. 1994. Enamel microstructure in Lemuridae (Mammalia. Primates): assessment of variability. Am J Phys Anthropol 95:221–241.

Maas MC, Dumont ER. 1999. Built to last: the structure, function, and evolution of primate dental enamel. Evol Anthropol 8:133–152.

Macho GA, Shimizu D. 2010. Kinematic parameters inferred from enamel microstructure: new insights into the diet of *Australopithecus anamensis*. J Hum Evol 58:23–32.

Macho GA, Shimizu D. 2009. Dietary adaptations of South African australopiths: inference from enamel prism attitude. J Hum Evol 57:241–247.

Macho GA, Spears IR. 1999. Effects of loading on the biochemical behavior of molars of *Homo*, *Pan*, and *Pongo*. Am J Phys Anthropol 109:211–227.

Mahoney E, Holt A, Swain M, Kilpatrick N. 2000. The hardness and modulus of elasticity of primary molar teeth: an ultra-micro-indentation study. J Dent 28:589–594.

Martin L. 1985. Significance of enamel thickness in hominoid evolution. Nature 314:260–263.

Martin LB, Boyde A, Grine FE. 1988. Enamel structure in primates—a review of scanning electron microscope studies. Scanning Microsc 2:1503–1526.

Martin LB, Olejniczak AJ, Maas MC. 2003. Enamel thickness and microstructure in pitheciin primates, with comments on dietary adaptations of the middle Miocene hominoid *Kenyapithecus*. J Hum Evol 45:351–367.

Millette JB, Sauther ML, Cuozzo FP. 2009. Behavioral responses to tooth loss in wild ring-tailed lemurs (*Lemur catta*) at the Beza Mahafaly Special Reserve, Madagascar. Am J Phys Anthropol 140:120–134.

Nash LT. 1998. Vertical clingers and sleepers: seasonal influences on the activities and substrate use of Lepilemur leucopus at Beza Mahafaly Special Reserve, Madagascar. Folia Primatol 69:204–217.

Oliver WC, Pharr GM. 1992. An improved technique for determining hardness and elastic-modulus using load and displacement sensing indentation experiments. J Mater Res 7:1564–1583.

Rand A. 1935. On the habits of some Madagascar mammals. J Mammal 16:89–104.

Robinson C, Kirkham J, Brookes SJ, Bonass WA, Shore RC. 1995. The chemistry of enamel development. Int J Dev Biol 39:145–152.

Sauther ML. 1998. Interplay of phenology and reproduction in ring-tailed lemurs: implications for ring-tailed lemur conservation. Folia Primatol 69:309–320.

Sauther ML, Cuozzo FP. 2009. The impact of fallback foods on wild ring-tailed lemur biology: a comparison of intact and anthropogenically disturbed habitats. Am J Phys Anthropol 140:671–686.

Sauther ML, Sussman RW, Cuozzo F. 2002. Dental and general health in a population of wild ring-tailed lemurs: a life history approach. Am J Phys Anthropol 117:122–132.

Schoeninger MJ, Iwaniec UT, Nash LT. 1998. Ecological attributes recorded in stable isotope ratios of arboreal prosimian hair. Oecologia 113:222–230.

Seligsohn D. 1977. Analysis of species-specific molar adaptations in Strepsirhine primates. Contrib Primatol 11:1–116.

Shaw GA. 1879. A few notes upon four species of lemurs, specimens of which were brought alive to England in 1878. Proc Zool Soc 47:132–136.

Shellis RP, Beynon AD, Reid DJ, Hiiemae KM. 1998. Variations in molar enamel thickness among primates. J Hum Evol 35:507–522.

Shimizu D, Macho GA. 2008. Effect of enamel prism decussation and chemical composition on the biomechanical behavior of dental tissue: a theoretical approach to determine the loading conditions to which modern human teeth are adapted. Anat Rec 291:175–182.

Simmen B, Sauther ML, Soma T, Rasamimanana HR, Sussman RW, Jolly A, Tarnaud L, Hladik A. 2006. Plant species fed on by *Lemur catta* in gallery forests of the southern domain of Madagascar. In: Jolly A, Sussman RW, Koyama N, Rasamimanana H, editors. Ring-tailed lemur biology. New York: Springer. p55–68.

Skedros JG, Bloebaum RD, Bachus KN, Boyce T, Constantz B. 1993. Influence of mineral-content and composition on gray-levels in backscattered electron images of bone. J Biomed Mater Res 27:57–64.

Spears IR. 1997. A three-dimensional finite element model of prismatic enamel: a re-appraisal of the data on the Young's modulus of enamel. J Dent Res 76:1690–1697.

Sussman R. 1974. Ecological distinctions in sympatric species of lemur. In: Martin RD, Doyle GA, Walker A, editors. Prosimian biology. London: Duckworth pp 75–108.

Tattersall I. 1982. Primates of Madagascar. New York: Columbia University Press.

Teaford MF. 2000. Primate dental functional morphology. In: Teaford MF, Smith MM, Ferguson MWJ, editors. Development, function, and evolution of teeth. Cambridge: Cambridge University Press. p290–304.

Teaford MF, Ungar PS. 2000. Diet and the evolution of the earliest human ancestors. Proc Natl Acad Sci 97:13506–13511.

Ungar PS. 1998. Dental allometry, morphology, and wear as evidence for diet in fossil primates. Evol Anthropol 6:205–217.

Ungar PS. 2002. Reconstructing the diets of fossil primates. In: Plavcan JM, Kay RF, Jungers WL, van Schaik CP, editors. Reconstructing behavior in the fossil record. New York: Kluwer Academic/Plenum Press. p261–296.

Ungar P. 2010. Mammal teeth. Baltimore: Johns Hopkins University Press.

Vajda EG, Skedros JG, Bloebaum RD. 1995. Consistency in calibrated backscattered electron images of calcified tissues and minerals analyzed in multiple imaging sessions. Scan Microsc 9:741–755.

Xie Z, Swain MV, Swadener G, Munroe P, Hoffman M. 2009. Effect of microstructure upon elastic behaviour of human tooth enamel. J Biomech 42:1075–1080.

Yamashita N. 1996. Seasonality and site specificity of mechanical dietary patterns in two Malagasy lemur families (Lemuridae and Indriidae). Int J Primatol 17:355–387.

Yamashita N. 1998. Functional dental correlates of food properties in five Malagasy lemur species. Am J Phys Anthropol 106:169–188.

Yamashita N. 2002. Diets of two lemur species in different microhabitats in Beza Mahafaly Special Reserve, Madagascar. Int J Primatol 23:1025–1051.

Yamashita N. 2003. Food procurement and tooth use in two sympatric lemur species. Am J Phys Anthropol 121:125–133.

Yamashita N. 2008. Food physical properties and their relationship to morphology: the curious case of *kily*. In: Vinyard CJ, Ravosa MJ, Wall CE, editors. Primate craniofacial function and biology. New York: Springer. p 387–406.

Yamashita N, Cuozzo FP, Sauther ML. in press. Interpreting food processing through dietary mechanical properties: a Lemur catta case study. Am J Phys Anthropol.

Zhou J, Hsiung LL. 2007. Depth-dependent mechanical properties of enamel by nanoindentation. J Biomed Mater Res A 81:66–74.